

**Time-Resolved FT-IR Spectroscopy of CO Hydrogenation over Supported
Ru Catalyst at 700 K**

Walter Wasylenko and Heinz Frei*

Physical Biosciences Division, MS Calvin Laboratory, Lawrence Berkeley

National Laboratory, University of California, Berkeley, CA 94720

HMFrei@lbl.gov

Abstract

Time-resolved FT-IR spectra of carbon monoxide hydrogenation over alumina-supported ruthenium were recorded on the millisecond timescale at 703 K using various H₂ concentrations (1 atm total pressure). Adsorbed carbon monoxide was detected along with gas phase products methane (3016 and 1306 cm⁻¹), water (sharp bands from 1900 – 1300 cm⁻¹), and carbon dioxide (2348 cm⁻¹). No other surface species were detected other than adsorbed carbon monoxide. The rate of formation of methane ($2.5 \pm 0.4 \text{ s}^{-1}$) coincides with the rate of formation of carbon dioxide ($3.4 \pm 0.6 \text{ s}^{-1}$), and bands due to water are observed to grow in over time. These results establish that methane and carbon dioxide originate from the same intermediate. The adsorbed carbon monoxide band is broad and unsymmetrical with a maximum at 2010 cm⁻¹ in spectra observed at 36 ms that shifts over 3000 ms to 1960 cm⁻¹ due to decreasing amounts of adsorbed carbon monoxide. Kinetic analysis of the adsorbed carbon monoxide band reveals that only a portion of the band can be temporally linked to gas phase products that we observe over the first 1000 ms of catalysis. This result suggests that we are observing dispersive kinetics, which is most likely due to heterogeneity of the surface environment.

1. Introduction

Mesoporous silica sieve of type MCM-41 has recently been employed as nanostructured high surface area support of single or binuclear transition metal sites for the photoreduction of CO₂ to CO. The material ZrCu^I-MCM-41 featuring binuclear Zr^{IV}-O-Cu^I centers on the pore surface affords splitting of adsorbed CO₂ to CO by photoexcitation of the metal-to-metal charge-transfer chromophore.¹ For this material, the resulting carbon monoxide is trapped inside the mesopores by coordinating to isolated Cu^I centers anchored on the silica surface. On the other hand, when conducting photoreduction of CO₂ gas by H₂O in TiMCM-41 sieve by single photon excitation of the Ti-O ligand-to-metal charge-transfer transition in the UV, gas phase CO is observed by in-situ FT-IR spectroscopy. Steady-state infrared monitoring of the photochemical reaction at room temperature does not reveal any adsorbed CO inside the material.² Yet, since the photoactivation of CO₂ takes place at Ti centers inside the pores, the CO product must reside, however brief, in the mesoporous channels before diffusing out of the pores into the gas phase. Clearly, molecular entities with high CO affinity present in the pores, as well as the specific micro- and mesostructure of these silicates may directly affect the diffusion properties of CO. The diffusion properties of CO, in turn may affect the performance of these mesoporous silicates in the photocatalytic reduction of CO₂ to CO. It is thus of interest to study the diffusion of CO in these materials.

2. Experimental Section

Time-resolved FT-IR spectra were recorded in the rapid-scan mode on a Bruker model IFS88 spectrometer equipped with a HgCdTe PV detector Kolmar Technologies model KMPV8-1-J2 (8 micron bandgap) or a HgCdTe PV detector model KMPV11-1-J2 (12 micron bandgap) as described previously.^{1,2} The method is described briefly below. The mirror velocity was 160 kHz, and the spectral resolution was 4 cm⁻¹. The protocol for obtaining the transient spectra consisted of the recording of 99 interferograms (double-sided/forward-backward) following a carbon monoxide pulse, corresponding to 396 single-sided interferograms. Single beam spectra obtained from the interferograms consisted of four 50 ms time slices followed by three 100 ms time slices, then a 10900 ms time slice, and the last time slice was 900 ms. A total of 50 such sets of single beam spectra generated by 50 carbon monoxide pulses were stored as the result of one experiment. Final time-resolved spectra for a given time delay were obtained by calculating the ratio of each of the 50 corresponding stored single beam spectra against the single beam spectrum taken just before the pulse. The 50 ratioed spectra were then averaged to yield the absorbance time slice for a given time delay. The results of 10 such experiments were averaged for further S/N improvement. Additional processing was performed with GRAMS/AI software Version 7.02, Thermo Electron including spectral deconvolution (gaussian bands, Levenburg-Marquardt method).

Slow runs on the time scale of seconds were conducted by a modified procedure. The method consisted of the recording of 396 interferograms following a carbon monoxide

pulse (double-sided/forward-backward at 160 KHz and 4 cm^{-1} resolution). The 99 interferograms were divided into 10 “buffers” at varying time resolution. The first two buffers were of 256 ms resolution (8 interferograms) followed by three buffers of 640 ms resolution (20 interferograms), one buffer of 1280 ms resolution (40 interferograms), one of 1920 ms resolution (60 interferograms), one of 2560 ms resolution (80 interferograms), one of 3840 ms resolution (100 interferograms), and the last buffer was of 1280 ms resolution (40 interferograms). Hence, the data stored after each carbon monoxide pulse consisted of 10 averaged interferograms taken at 128, 384, 832, 1472, 2112, 3072, 4672, 6912, 9792, 12032 ms after the reactant pulse (midpoints).

The Al_2O_3 -supported, Ru catalyst (Aldrich, 5% Ru, Degussa type H213 R/D, BET surface area $96\text{ m}^2\text{g}^{-1}$) was prepared in the form of a pressed wafer with an embedded W grid. The latter is made of a 0.49 in. diameter tungsten foil (thickness 0.002 in.) featuring laser-drilled 0.012 in. holes. The grid, which was held by a Ni jaw similar to a design described by Yates³ was electrically heated and the temperature monitored by a thermocouple mounted on the W grid. The catalyst was situated in the center of home built 100 cm^3 stainless steel reactor cell equipped with two flange-mounted BaF_2 windows for transmission infrared spectroscopy. The catalyst was transparent in the region $5000\text{--}800\text{ cm}^{-1}$ (reduced sensitivity below 1100 cm^{-1} because of Al-O stretch absorption). The continuous flow of a H_2/N_2 mixture (ratio 0.067 or 0.15) with a flow of either 4.5 L/min or 5.4 L/min at a total pressure 1 atm entered the cell through a $\frac{1}{4}$ in. tube on one side and exited through an exhaust line on the other. The flow of each gas was regulated by MFC valves (MKS Instruments). Millisecond time resolution was

achieved by the synchronization of carbon monoxide pulses of 30 ms duration with the forward motion of the interferometer mirror.² The spacing between carbon monoxide pulses was 12.8 s, which assured that all reaction had ceased prior to arrival of a fresh pulse. The pulses were released through a fast valve (General Valve Series 99 pulsed valve coupled with an Iota One pulse driver) and contained 15 micromol carbon monoxide. The pulses merged with the continuous H₂/N₂ flow 7 cm upstream from the center of the reactor cell. Before each series of experiments, the Ru/Al₂O₃ catalyst was exposed for six hours to a H₂/N₂ flow at 600 K and the for one hour at 703 K in order to assure complete reduction of the Ru surface. Carbon Monoxide (Air Gas, 99.99%), hydrogen (Air Gas, 99.9999%), hydrogen in nitrogen (Airgas, H₂/N₂ ratio 0.15), deuterium (Isotec, 99.8 % D), and nitrogen (Air Gas, 99.9995%) gas were used as received.

3. Results and Discussion

The transient spectra observed following the initiation of catalysis on Ru/Al₂O₃ at 703 K with a carbon monoxide pulse are displayed in Figure 1. The first three traces are 50 ms resolution, the fourth is 100 ms, and the fifth is recorded over several seconds. The bottom trace is the first spectrum observed, with its midpoint delayed by 36 ms relative to the opening of the pulsed carbon monoxide valve. Subsequent traces are shown at 95, 223, 577, and 6000 ms. The most prominent bands are due to gas phase carbon monoxide, centered around 2143 cm⁻¹.⁴ As shown in Figure 2, gas phase carbon

monoxide band remains constant over the first 300 ms and then decreases, principally due to removal of reactant from the infrared viewing zone by gas flow.^{5,6}

In addition to gas phase carbon monoxide, bands are observed at 3016, 2348, 2010, and 1306 cm^{-1} (Figure 1). The most intense of these bands (2010 cm^{-1}) is unsymmetrical and does not completely return to baseline till around 1500 cm^{-1} . This band is assigned to adsorbed carbon monoxide based on previous infrared studies.⁷⁻¹⁷ The other bands are due to gas phase products methane (3016 and 1306 cm^{-1}) and carbon dioxide (2348 cm^{-1}), based on comparison to static spectra and previous studies.⁴ Also, a series of sharp bands in the 1900 – 1300 cm^{-1} region are observed and assigned to gas phase product water. Bands due to gas phase products are displayed on expanded scales in Figure 3 and 4. Other than the species described so far, no other bands are present in any of the transient spectra.

The adsorbed carbon monoxide band possesses the strongest absorbance shortly after the initiation of catalysis and decreases over time. This decrease is accompanied by a red shift from 2010 cm^{-1} at 36 ms to 1990 cm^{-1} at 897 ms. In addition, the band broadens, especially around the peak position as seen in Figure 5. In data obtained after 1 s (Figure 6) the red shift of the band continues till 3072 ms where the maximum shifts to 1960 cm^{-1} , which is consistent with earlier reports.^{8,18} Also, of note is that in the 6912 ms trace a signal due to adsorbed CO is no longer observed, providing considerable evidence that reaction is complete prior to the introduction of a fresh pulse of CO(g). Due to the red shift and broadening of the adsorbed carbon monoxide, the kinetics are examined by two

methods. The first consists of taking the whole band with max absorbance near 2010 cm^{-1} and determining its area (mass of band from 2075 cm^{-1} to 1650 cm^{-1}). The global decay, shown in Figure 7 for 0.067 H_2/N_2 ratio, is nearly constant over the first 1500 ms, and then is found to decay over several seconds. The second method only considers the portion of the adsorbed CO band that corresponds to the bleach at early times ($< 1\text{ s}$). As can be seen from the difference spectra in Figure 8, the bleach remains centered at 2026 cm^{-1} for the first 600 ms of the reaction. Therefore, a spectral deconvolution of the profile of adsorbed CO is conducted with one Gaussian component fixed at 2026 cm^{-1} (GRAMS/AI software). The result of deconvolution and the kinetics of the decay are displayed in Figure 9. The calculated best fits to a single-exponential function gives a rate constant of $2.9 \pm 0.1\text{ s}^{-1}$ (0.067 H_2/N_2 ratio, 4.5 L/min flow). As can be seen from Figure 10, this is the same within uncertainties as the rise constant of the methane ($2.5 \pm 0.4\text{ s}^{-1}$) and carbon dioxide products.

Determination of the best fit to the kinetic data of gas phase products, CH_4 and CO_2 , required that the data be fit using a modified exponential equation due to the loss of product by removal through gas flow. These processes can be represented by equation 1 where R is carbon monoxide, P is gas phase product in the IR viewing zone, and P' is gas phase product removed from viewing zone by gas flow.



$$\frac{d[\text{P}]}{dt} = k_1[\text{R}] - k_2[\text{P}] \quad (2)$$

$$A^P = A \frac{\varepsilon^P}{\varepsilon^{P'}} \frac{k_1}{k_2 - k_1} \left(\exp(-k_1^*t) - \exp(-k_2^*t) \right) \quad (3)$$

Using this hypothesis the growth and decay of the gas phase products can be fit using the kinetic model^{19,20} of equations 2 and 3 where $[P]$ is the concentration of gas phase product (P) in the IR viewing zone at time t , $[R]$ is the concentration of R at time t , A^P is the absorbance of P at time t , A is the asymptotic absorbance of P', and ε^P and $\varepsilon^{P'}$ are the IR extinction coefficients at frequencies being monitored of P and P' respectively. The growth of the two methane bands is the same within uncertainties, with $k_1 = 2.5 \pm 0.4 \text{ s}^{-1}$ (0.067 H₂/N₂ ratio, 4.5 L/min flow). The rate of growth (k_1) for carbon dioxide under the same H₂ concentration and flow conditions is $3.4 \pm 0.6 \text{ s}^{-1}$, which is the same rate that was found for methane indicating that these two products originate from the same intermediate. In addition, k_2 determined for both methane ($0.52 \pm 0.07 \text{ s}^{-1}$) and carbon dioxide ($1.2 \pm 0.2 \text{ s}^{-1}$) are in general agreement with the rate determined for the removal of gas phase carbon monoxide (see Figure 2). While quantitative data for the growth kinetics for water could not be obtained because of lack of spectral resolution, the ro-vibrational bands grow in slowly over a few hundreds of ms. Based on comparison with authentic spectra, the ratio of the asymptotic methane and carbon dioxide is 0.44 (0.15 H₂/N₂ ratio, 4.5 L/min flow, assuming rate of production of CH₄ and CO₂ are the same) [this needs to be done because when H₂/N₂ ratio is 0.15 I cannot use eq 3 to obtain good values for k_1 and k_2 for CO₂, so I fit the CO₂ data by fixing k_1 to the value found for methane (avg of 3016 and 1306 cm⁻¹ bands). I have included in the paper copy both fits] and 0.17 (0.067 H₂/N₂ ratio, 4.5 L/min flow). These results indicate that under our experimental conditions that carbon dioxide is a significant product. [may also need to

recalculate these due to the fact that I used A in eq 3 to obtain these values and did not find “A_p” at [P_{max}]]

When D₂ (D₂/N₂ ratio- 0.067 and 4.5 L/min flow) is used instead of H₂ the spectra that are observed following initiation of catalysis are consistent with what was observed with H₂ except that signals due to CH₄ (3016 and 1306 cm⁻¹) are replaced with new bands at 2256 and 993 cm⁻¹ (data not shown). The bands agree with the ν_3 and ν_4 modes of CD₄ when compared to literature values.⁴ A comparison of the growth rate of the 2256 cm⁻¹ band with experiments using H₂ where the same H₂/N₂ ratio and flow are used produces a kinetic isotope effect (KIE, k_H/k_D) of 1.1.

4. Conclusions

Time-resolved rapid-scan FT-IR spectra of carbon monoxide hydrogenation over alumina-supported ruthenium nanoparticle catalyst were recorded at 700 K under various H₂ concentrations. The catalyst was prepared in the form of a waiver pressed into a tungsten grid for heating, and measurements were conducted in the transmission mode. Reactants were delivered to the catalyst by a continuous H₂/N₂ flow (7 to 15%, flow range 4.5 to 9 L min⁻¹) into which a ms pulse of CO was released upstream from the catalyst. The buildup of adsorbed CO on the catalyst surface is complete at 30 ms after the release of the reactant pulse. The initial absorption peaks at 2010 cm⁻¹ and shows a very long tail extending to 1500 cm⁻¹. Growth of gas phase methane (3016 and 1306 cm⁻¹; CD₄: 2256 and 993 cm⁻¹), water (series of ro-vibrational bands 1900 – 1300 cm⁻¹), and

carbon dioxide product (2348 cm^{-1}) was observed on the hundreds of ms time scale. The rate of formation of CH_4 ($2.5 \pm 0.4\text{ s}^{-1}$) coincides with the growth of CO_2 ($3.4 \pm 0.6\text{ s}^{-1}$), indicating that both species originate from a common precursor. The rate was found to agree with the decay rate of the high frequency component (centered at 2010 cm^{-1}) of the broad surface CO absorption. This reveals that dissociation of CO is the rate determining step of the reaction and explains the absence of infrared bands of other surface intermediates in infrared region ($4000 - 800\text{ cm}^{-1}$). Furthermore, the position of the band indicates that the most reactive CO molecules are weakly bound to the metal surface. At times beyond 1000 ms, the absorption maximum of adsorbed CO shifts gradually to the red (at 1960 cm^{-1} at 3000 ms), mostly caused by the decreasing surface concentration of carbon monoxide. Analysis of the temporal behavior of the adsorbed CO across the entire decay (complete after 7 s) reveals dispersive kinetics, which manifests differences in the reactivity of the various adsorption sites. The kinetic isotope effect (CH_4/CD_4) of 1.1 at the temperature used is in agreement with earlier work by steady state infrared or MS monitoring.

Acknowledgment

This work was supported by the Director, Office of Science, Office of Basic Energy Sciences, Division of Chemical, Geological and Biosciences of the U.S Department of Energy under contract No. DE-AC03-76SF00098.

References

- (1) Yeom, Y. H.; Frei, H. *J. Phys. Chem. A* 2002, *106*, 3350-3355.
- (2) Yeom, Y. H.; Frei, H. *In-Situ Spectroscopy of Catalysts* 2004, 32-46.
- (3) Basu, P.; Ballinger, T. H.; Yates, J. T., Jr. *Rev. Sci. Instrum.* 1988, *59*, 1321-1327.
- (4) Herzberg, G. *Infrared and Raman Spectra of Polyatomic Molecules*; D. Van Nostrand Co.: New York, 1945.
- (5) Ko, M. K.; Frei, H. *J. Phys. Chem. B* 2004, *108*, 1805-1808.
- (6) Wasylenko, W. A.; Frei, H. *J. Phys. Chem. B* 2005, *109*, 16873-16878.
- (7) Dalla Betta, R. A.; Shelef, M. *J. Catal.* 1977, *48*, 111-119.
- (8) Ekerdt, J. G.; Bell, A. T. *J. Catal.* 1979, *58*, 170-187.
- (9) Gupta, N. M.; Kamble, V. S.; Iyer, R. M.; Thampi, K. R.; Gratzel, M. *J. Catal.* 1992, *137*, 473-486.
- (10) Kantcheva, M.; Sayan, S. *Catal. Lett.* 1999, *60*, 27-38.
- (11) Kellner, C. S.; Bell, A. T. *J. Catal.* 1981, *71*, 296-307.
- (12) McQuire, M. W.; Rochester, C. H. *J. Catal.* 1993, *141*, 355-367.
- (13) Nawdali, M.; Ahlafi, H.; Pajonk, G. M.; Bianchi, D. *J. Mol. Catal. A* 2000, *162*, 247-256.
- (14) Pfnuer, H.; Menzel, D.; Hoffmann, F. M.; Ortega, A.; Bradshaw, A. M. *Surf. Sci.* 1980, *93*, 431-452.
- (15) Pien, S. I.; Chuang, S. S. C. *J. Mol. Catal.* 1991, *68*, 313-330.
- (16) Todorova, S. Z.; Kadinov, G. B. *Res. Chem. Intermed.* 2002, *28*, 291-301.

- (17) Yamasaki, H.; Kobori, Y.; Naito, S.; Onishi, T.; Tamaru, K. *J. Chem. Soc., Faraday Trans. 1* 1981, 77, 2913-2925.
- (18) Cant, N. W.; Bell, A. T. *J. Catal.* 1982, 73, 257-271.
- (19) Atkins, P. W. *Physical Chemistry*; 5th ed.; W. H. Freeman: New York, 1994.
- (20) Nakata, M.; Frei, H. *J. Amer. Chem. Soc.* 1989, 111, 5240-5247.

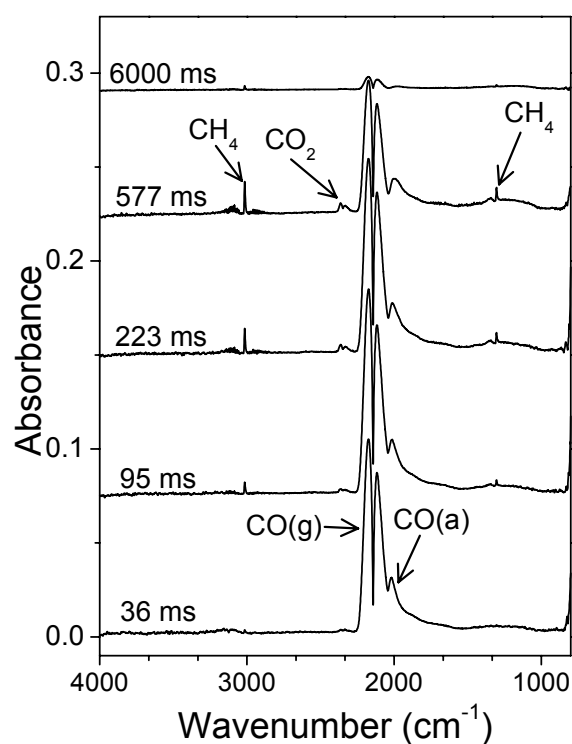


Figure 1. Rapid-scan survey spectra of CO + H₂ reaction induced by carbon monoxide pulses over Ru/Al₂O₃ at 703 K (0.15 H₂/N₂ ratio, 5.4 L/min flow) consisting of 3 time slices of 50 ms, one of 100 ms, and the last recorded over several seconds at 4 cm⁻¹ resolution. Times refer to the time delay between the opening of the pulsed valve and the midpoint of the corresponding interferogram slice. Gas phase carbon monoxide is CO(g) and adsorbed carbon monoxide is CO(a). Small transient bands are shown on an expanded scale in Figures 3 – 6.

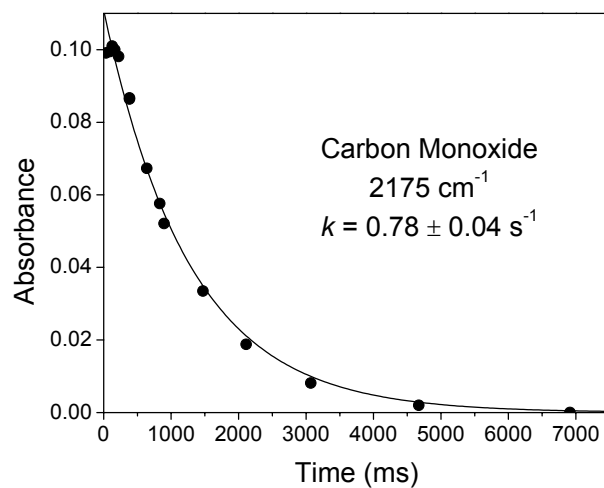


Figure 2. Decrease of carbon monoxide absorption (peak intensity of the 2175 cm^{-1} band) caused by gas flow. A CO pulse of 30 ms duration (85 psi back pressure) was released into a continuous $\text{H}_2\text{-N}_2$ flow (0.67 H_2/N_2 ratio, 5.4 L/min flow). The solid line represents a best fit using a single exponential function.

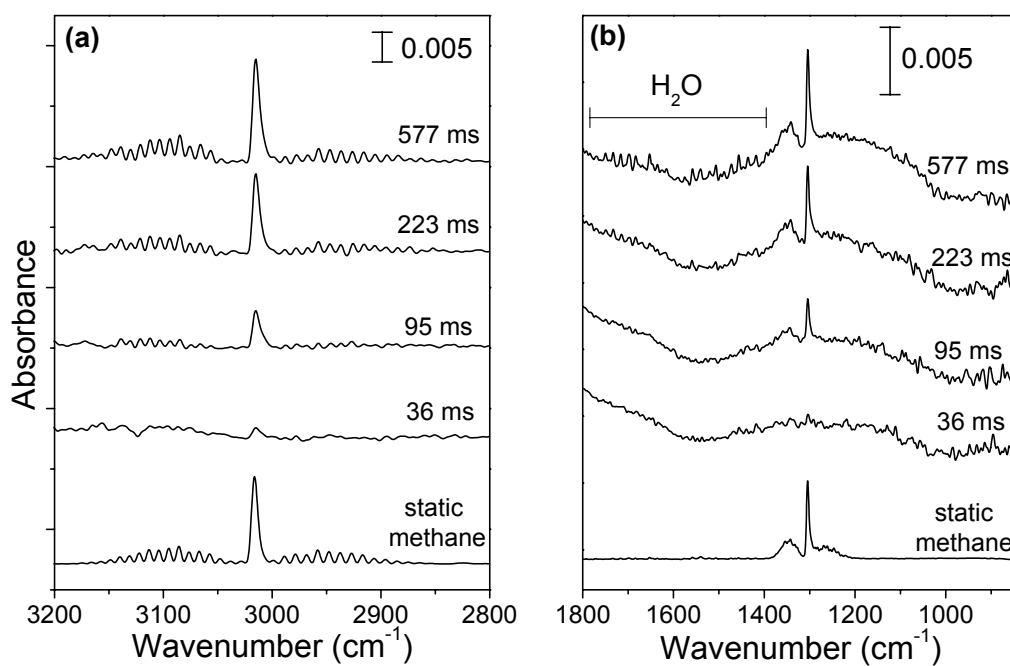


Figure 3. Rapid-scan spectra (4 cm^{-1} resolution) in the (a) $3200\text{--}2800\text{ cm}^{-1}$ and (b) $1800\text{--}800\text{ cm}^{-1}$ regions observed following the initiation of $\text{CO} + \text{H}_2$ catalysis at 703 K ($0.15\text{ H}_2/\text{N}_2$ ratio, 5.4 L/min flow). The bottom trace shows the static spectrum of an authentic methane sample recorded with the same spectral parameters used for the time-resolved $\text{CO} + \text{H}_2$ runs.

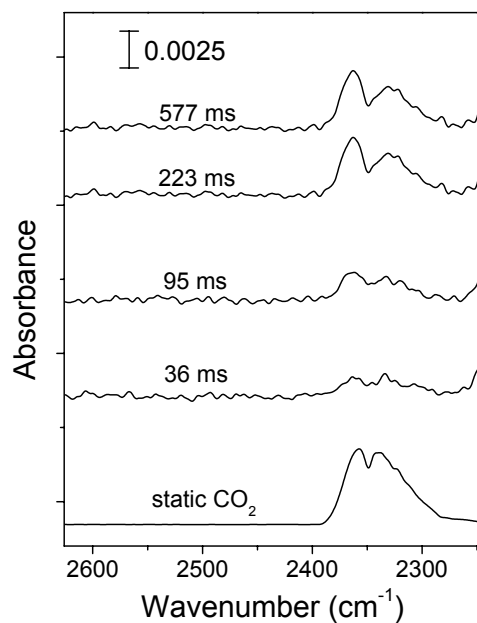


Figure 4. Rapid-scan spectra (4 cm^{-1} resolution) in the $2625\text{--}2250 \text{ cm}^{-1}$ region observed following the initiation of $\text{CO} + \text{H}_2$ catalysis at 703 K ($0.15 \text{ H}_2/\text{N}_2$ ratio, 5.4 L/min flow). The bottom trace shows the static spectrum of an authentic carbon dioxide sample recorded with the same spectral parameters used for the time-resolved $\text{CO} + \text{H}_2$ runs.

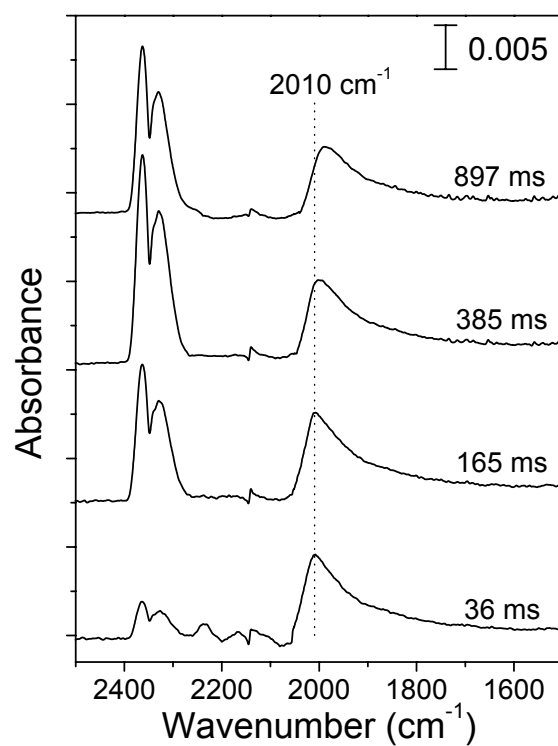


Figure 5. Rapid-scan spectra (4 cm^{-1} resolution) in the $2500\text{--}1500 \text{ cm}^{-1}$ region observed following the initiation of $\text{CO} + \text{H}_2$ catalysis at 703 K ($0.067 \text{ H}_2/\text{N}_2$ ratio, 4.5 L/min flow) during the first 1000 ms . The gas phase bands due to carbon monoxide have been subtracted.

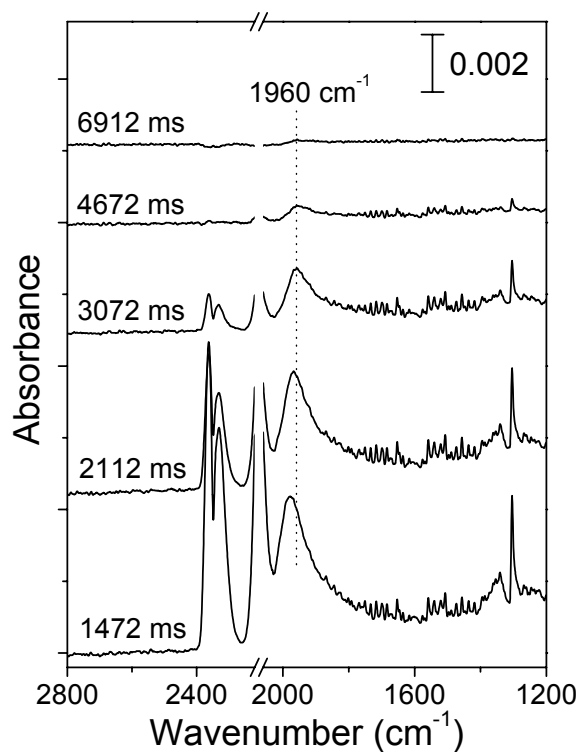


Figure 6. Rapid-scan spectra (4 cm^{-1} resolution) in the $2800\text{--}1200 \text{ cm}^{-1}$ region observed following the initiation of $\text{CO} + \text{H}_2$ catalysis at 703 K ($0.067 \text{ H}_2/\text{N}_2$ ratio, 4.5 L/min flow) displaying decay of adsorbed carbon monoxide from 1150 ms to 8000 ms . Data due to CO(g) between 2220 and 2060 cm^{-1} is not shown.

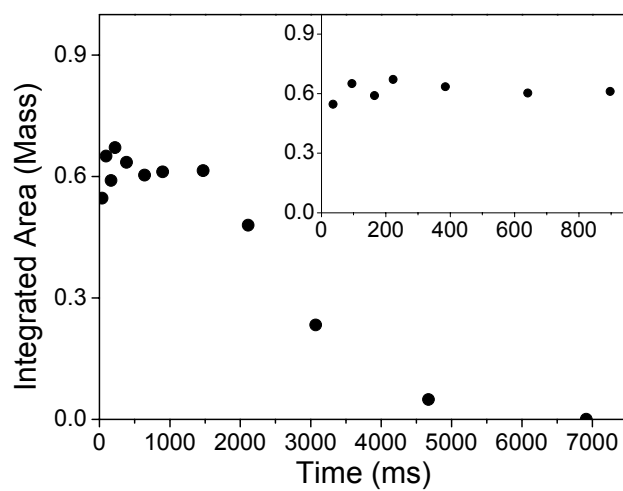


Figure 7. Kinetics of the adsorbed carbon monoxide observed following the initiation of CO + H₂ catalysis at 703 K (0.067 H₂/N₂ ratio, 4.5 L/min flow). Integrated area is determined by the mass of band from 2050 cm⁻¹ to 1650 cm⁻¹. The inset shows the first 1000 ms on an expanded scale.

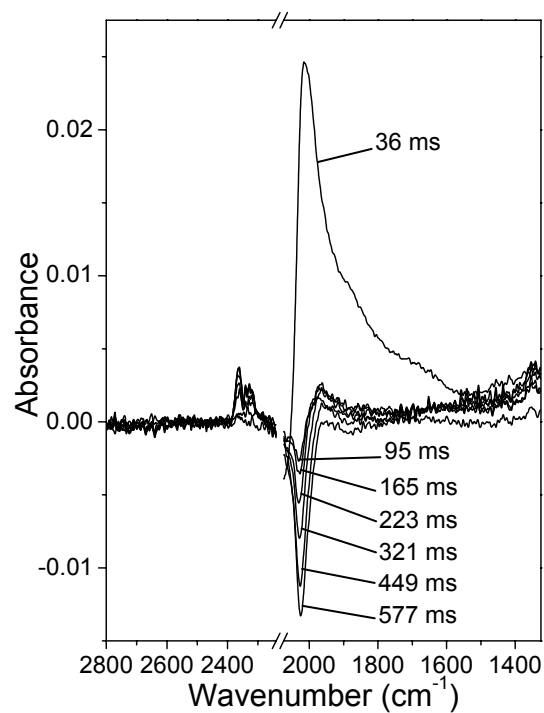


Figure 8. Difference spectra ($\text{time}_i - 36 \text{ ms}$ trace) in the C=O region which reveals the bleach at 2026 cm^{-1} due to adsorbed carbon monoxide. The 36 ms trace following the initiation of CO + H₂ catalysis at 703 K is also displayed (0.15 H₂/N₂ ratio, 5.4 L/min flow). The gas phase bands due to carbon monoxide have been subtracted. The area around the gas phase carbon monoxide is not displayed.

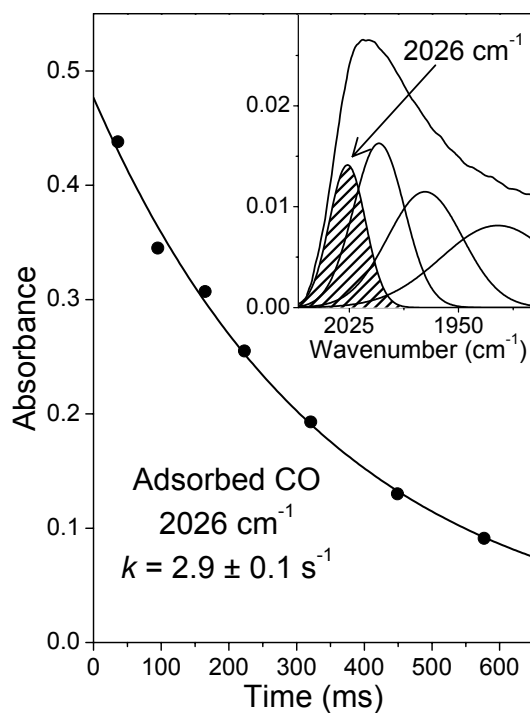


Figure 9. Kinetics of adsorbed carbon monoxide (integrated area of 2026 cm⁻¹ band, see text) observed following the initiation of CO + H₂ catalysis at 703 K (0.067 H₂/N₂ ratio, 4.5 L/min flow). The solid line represents a best fit using a single exponential function. The inset shows the component bands resulting from a spectral deconvolution (GRAMS/AI software) of the 36 ms trace.

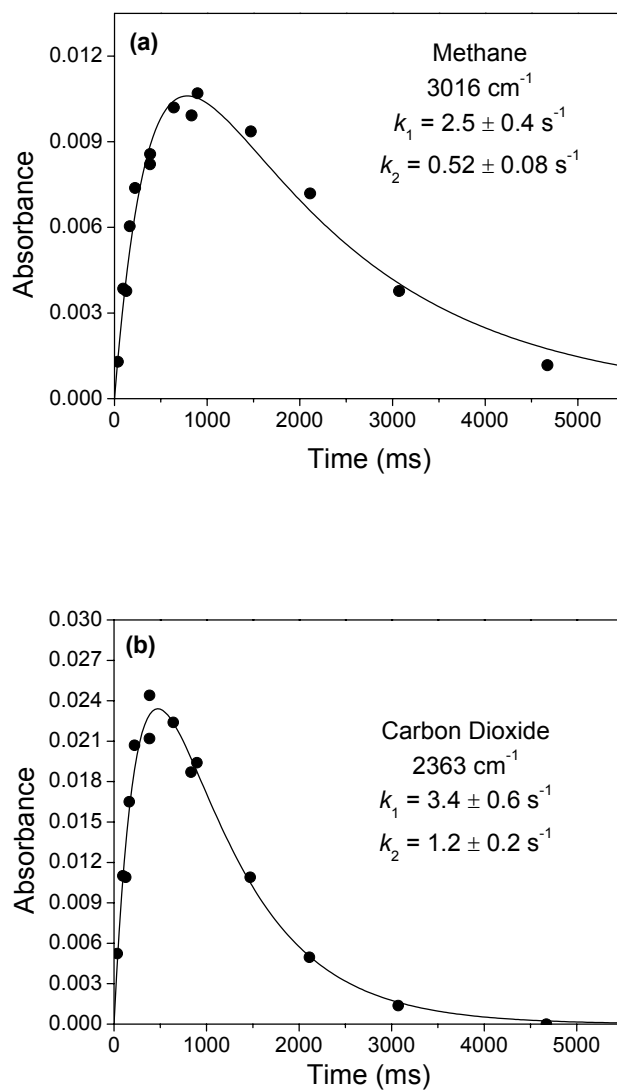


Figure 10. Kinetics observed for gas phase products (a) methane (peak absorbance at 3016 cm^{-1}) and (b) carbon dioxide (peak absorbance at 2363 cm^{-1} from the 2348 cm^{-1} band) following the initiation of CO + H₂ catalysis at 703 K (0.067 H₂/N₂ ratio, 4.5 L/min flow). The solid lines represent best fits using equation 3 in each plot.